JOURNAL OF SOLID STATE CHEMISTRY 117, 219–228 (1995)

Structural Evolution from Tin Sulfide (Selenide) Layered Structures to Novel 3- and 4-Connected Tin Oxy-sulfides

John B. Parise,*,†,[1] Younghee Ko,* Kemin Tan,* David M. Nellis,† and Stephen Koch†

*CHiPR[2] and Department of Earth and Space Sciences, State University of New York, Stonybrook, New York, 11794-2100; and †Department of Chemistry, State University of New York, Stonybrook, New York, 11794-3400

Received August 30, 1994; accepted November 5, 1994

Addition of triethylenetetramine (TETN) and tetramethylammonium (TMA^+) to SnS_2 and $SnSe_2$ slurries followed by heating at 150°C under autogenous hydrothermal conditions results in novel thio and thio-oxide phases. These materials crystallize in time sequence as the added amines decompose. Initially 2-D frameworks with composition $(Sn_3X_7)^{2-}$, X = S or Se are produced. In the case of the sulfides these are shown to transform to 2-D and 3-D oxy-sulfides frameworks which incorporate the decomposed template. The structures of two materials in this sequence have been determined from single crystal X-ray diffraction. The first, $Sn_3Se_7 \cdot C_6N_4H_{16}CO$, designated TETN–SnSe-1, crystallizes after 1 day of digestion in space group *Pbca*, with a = 23.553(6), b = 14.004(6), and c = 13.967(4) Å. The structure contains $SnSe_5$ coordination polyhedra which form $Sn_3Se_4^{4+}$ semicubes; six such semicubes are linked via Se_2 bridges to form apertures in the $Sn_3Se_7^{2-}$ sheet in (010). Similar structures occur in the TETN–SnS and TMA–SnS systems. The second material, with a framework designated SnOS-SB3, is formed after 5 days of digestion in either the TMA–SnS or TETN–SnS systems and crystallizes in $C2/c$, with a = 35.62(1), b = 18.468(4), c = 21.858(6) Å, and β = 115.36(1)°. The structure consists of tetrahedral clusters of composition $[Sn_{10}S_{20}O_4]^{8-}$, which are linked via single S bridges at three corners to form a 2-D framework of composition $[Sn_{20}S_{37}O_8]^{10-}$. This is one member of a theoretical structural family with composition $[Sn_{10}S_{20-n/2}O_4]^{(8-n)-}$, where $0 \le n \le 4$ and represents the number of connections between clusters.

INTRODUCTION

We recently reported the first example of a 4-connected oxy-sulfide network (1). This material share structural characteristics associated with both tetrahedral oxide frameworks and with isolated sulfide clusters. Tetrahedral clusters of composition $[Sn_{10}S_{20}O_4]^{8-}$ are connected to one another through four sulfur bridges to form a 3-D net similar to that found in the cristobalite polymorph of silica. We suggested (1, 2) that this framework might be one member of a family possessing a structural chemistry analogous to that found in the silicates (3). We report here two new thio-oxide materials; one is consistent with our prediction and possesses a sheet structure, reminiscent of those tetrahedral sheets found in the clays and micas. The other represents a possible link between the sulfides, which are the first to crystallize from our hydrothermal preparations, and the oxy-sulfide networks into which they evolve after prolonged digestion.

Open crystalline structures, possessing regularly spaced pores and channels, offer a number of features of sufficient potential interest and utility to warrant exploratory synthesis. For example, since diffusion of molecular and ionic species would be facile, framework structures of this type should show interesting selective molecular sieving, catalytic, ion exchange, and ion conductive properties. The compositional and structural range of materials capable of forming open frameworks has increased greatly over the past decade. Based upon experience with the hydrothermal synthesis of zeolites (4–7) silicon in the prototypical SiO_2 framework was replaced by "III–V" elements to form neutral 4-connected networks based upon the chemistries $AlPO_4$ (8–12) and $GaPO_4$ (13, 14). Further exploratory studies uncovered charged and neutral frameworks of main group elements (15) along with networks incorporating transition elements (16–20). Less-crystalline microporous materials have been produced from pillaring of layered silicates and phosphates (21). The materials cited above are all oxides.

The inspiration for much of this work comes from the mineralogy, synthesis, and structural chemistry of the zeolites. These are solids in which SiO_4- and AlO_4-tetrahedra share all four apical oxygens (i.e., are 4-connected (9, 22) to produce open frameworks.) When synthesized in the presence of alkali earth metals and/or organic cations (4–6) frameworks constructed from tetrahedral or octahedral centers often generate a regular array of cavities, interconnected by windows. The size of these cavities and windows will in general be larger in the 4-connected

[1] To whom correspondence should be addressed.

[2] Center for High Pressure Research: NSF funded Science and Technology Center.

0022-4596/95 $12.00

tetrahedral case (22) and often reflect the geometry of the added organic or alkali metal hydration environment. This observation is suggestive of a templating mechanism whereby the additives serve to organize the self-assembly of complex frameworks from simple starting materials (6, 7, 23).

The aluminosilicate family (3) is an excellent example of the variety of structure types which are available when tetrahedral centers can be induced to form isolated (nesosilicates such as olivine), 1-connected (sorosilicates such as epidote), 2-connected (ionosilicates such as pyroxene), 3-connected (sheet silicates such as the micas and clays), and 4-connected structures (silicas and zeolites). Because of their commercial applications as catalysts, detergent builders, ion exchangers, and in separations technologies (24, 25), the aluminosilicate zeolites are the most studied of the 4-connected networks. More recently, these crystalline solids have been employed for "ship-in-a-bottle" type chemistry in which a particular pore structure (26) is employed to stabilize unique compounds or pieces of extended structure within their cavities (27–30). Their importance in industry and their increasing use in innovative chemistry are a consequence of their selectivity toward reactant, product, and transition state. These properties are intimately connected to their crystalline structures, which consist of regular arrays of pores and channels about the size of common organic molecules. Further, their selectivity can be fine-tuned by choosing a particular molecular sieve from those cataloged (26), by modifying them (31), or by synthesizing new ones. Of primary importance in these studies is the determination of crystal structure; once this is known, sensible predictions of which reactants, products, and transition states will be likely within a particular molecular sieve can be made.

We have been synthesizing and characterizing novel thio- and thio-oxide-based frameworks and determining their properties. Following upon earlier reports of sulfide frameworks (2, 32–46) and their potential (28, 29), we have worked at determining the structures of our own novel materials as well as those reported in the original Carbide patent (40, 42). Microporous sulfide frameworks represent a new class of solid (40) and a significant departure from the oxide chemistry on which other crystalline molecular sieves are based. As was first pointed out by Bedard *et al.* (40–42), the sulfides possess a richer metal-coordination chemistry (47) and a propensity to form 3- and 4-rings (26, 40) and rigid *M*–S–*M* linkages, which connect the building units of the framework; the latter two differences can lead to more open structures with larger cavities.

The methodology for the synthesis of molecular sieves has been reviewed elsewhere (4–7, 23, 48). Typically, all starting materials are slurried, with a structure directing agent added prior to heating under autogenous pressure to produce a crystalline phase. This structure directing agent or template, is typically an amine. The details of nucleation, growth, and the effect of added template on the gel are areas of active study; some progress is reported from small angle neutron scattering (49) and in the syntheses "designed" to produce chiral materials (7). However, serendipity remains a powerful ally in exploratory syntheses in this area. We have found a series of phases (1, 46, 50) are produced in time sequence for certain templates and have some evidence for the transformation from thio to thio-oxide frameworks being related to the breakdown of the added amine. For example in the TMA–SnS system, the breakdown of TMA^+ leads to the formation of a collapsed layer structure (51) and eventually to the formation of the three-dimensional oxy-sulfide network (1). The TETN–SnS-system behaves in a similar fashion. By determining the structures of these metastable intermediates we hope to learn about the transformation mechanism involved in this chemistry. We report here two frameworks formed when triethylenetetramine (TETN) and tetramethylammonium (TMA^+), molecules known to breakdown under the conditions normally used in molecular sieve synthesis (52), are added to SnS_2 and $SnSe_2$ slurries.

Synthesis

TETN–SnSe-1. Single crystals of all the phases reported here were produced in the manner described in previous publications (1, 43–46, 50, 51, 53, 54). Slurries of $SnSe_2$, triethylenetetramine, elemental selenium, and H_2O, in a mole ratio of 3 : 2 : 2 : 30, were heated at 150°C for 4 days under autogenous hydrothermal conditions in Pyrex-lined bombs. Yields were low compared to the sulfide system, 30% based on $SnSe_2$. Samples included uncreacted $SnSe_2$ starting material. The elemental selenium was dissolved completely in TETN prior to mixing with the other components. During this process, TETN absorbed CO_2 from the atmosphere; the solubility of CO_2 in H_2O at room temperature is 0.145 g per 100 cc. An infrared spectrum from a sample of the TETN–Se mixture showed a peak at 2350 cm^{-1} due to asymmetrical stretching vibration of CO. Reaction of CO_2 with TETN, followed by treatment under heat and pressure, is known to lead to the formation of 1,3-aminoethyl 2-imidazolidone (55). The presence of this product was confirmed in a subsequent crystallographic study.

An X-ray powder diffraction pattern for TETN–SnSe-1 was compared with that of the sulfide crystallized from TETN/SnS_2/S-slurries after 2 days at 150°C. Apart from some impurities attributed to $SnSe_2$ contamination in the pattern of the former compound, the peak positions and relative intensities suggested that the two phases are isomorphous.

TABLE 1
Summary of X-Ray Diffraction Data for TETN–SnSe-1 and TMA–SnO-SB3

Compound	$(C_7N_4OH_{16})_2 \cdot Sn_3Se_7 \cdot H_2$ TETN–SnSe-1	Framework $[Sn_{20}S_{37}O_8]^{10-}$ TMA–SnOS-SB3[a]
Formula weight	1136.02	3688.64
Crystal	Orange, 0.20 × 0.05 × 0.10 mm	Colorless, 0.07 × 0.05 × 0.04 mm
Space group	*Pbca*	*C2/c*
a (Å)	23.553 (6)	35.62 (1)
b (Å)	14.004 (6)	18.468 (4)
c (Å)	13.967 (4)	21.858 (6)
β (°)		115.36 (1)
Volume (Å^3)	4607 (4)	12992 (6)
Z	8	4
ρ_{calc} (g cm^{-3})	3.172	1.984[a]
μ (mm^{-1})	13.0	4.37[a]
Temperature	Ambient	
λ (Mo$K\alpha$) (Å)	0.71073	
Scan mode	$\omega/2\theta$	
Max θ (°)	27	22
Standard reflections	1 measured every 20 reflections	
Reflections collected	3518	6313
Uniques with $\lvert F_0\rvert > 3\sigma\lvert F_0\rvert^2$	2203	5035
R_{merge}	2.48	2.81
Absorption correction	DIFABS	
Parameters refined	217	307
Data/parameter ratio	10.2	16.4
Agreement factors[c] R (R_w)	0.042 (0.041)	0.072 (0.060)
Weighting scheme	$w = [\sigma^2(I) + 0.0009*I^2]^{-1/2}$	
Std. error in obs. of unit wt.	1.15	1.14
Δ/σ_{max}	0.03	0.03

[a] Inferred from structure determination; interlayer cations presumed to be breakdown products of TMA and to be disordered over the space between the SnOS layers.
[b] See Ref. (63).
[c] $R = \Sigma(\lvert F_0\rvert - \lvert F_c\rvert)/\Sigma(\lvert F_0\rvert$; $R_w = [\Sigma w(\lvert F_0\rvert - \lvert F_c\rvert)^2/\Sigma w(\lvert F_0\rvert^2]^{1/2}$.

TMA–SnOS-SB3. Slurries of SnS_2, tetramethylammonium hydroxide (TMAOH), elemental sulfur, and H_2O were produced in a mole ratio of 3 : 2 : 2 : 30 and then heated at 180°C for 14 days under autogenous hydrothermal conditions in Pyrex-lined bombs. Yields were 85% based on SnS_2. The TMAOH was reacted completely with elemental sulfur prior to mixing with the other components. Similar conditions were used to synthesize TETN–SnS-SB3, which has a similar X-ray powder diffraction pattern to the TMA compound.

Structure Determination

TETN–SnSe-1. A single crystal of this phase was chosen for data collection from a preparation that had been allowed to react for about 16 hr. The sample contained considerable quantities of unreacted $SnSe_2$ as well as well-formed crystals up to 0.3 mm on edge. A summary of the crystal data is given in Table 1. The structure was solved using an automated Patterson search routine (56) written by Calabrese of the DuPont Company. Subsequent least-squares refinement followed by the calculation of Fourier difference maps revealed the SnSe layers (Fig. 1) and the backbone of the template molecule (Figs. 2 and 3) occluded within this framework. The geometry of this molecule, along with the chemistry expected for the TETN added to the reaction mixture prior to heating (55), was used as a basis for the assignment of C, N, and O atoms in the template. The assignment of an oxygen atom (O(2) in Fig. 2) was made on the basis of the planarity of the template; the atoms O(2), N(2), N(3), and C(7) in Fig. 2 are within 0.01 Å of the mean plane calculated from the coordinates of these atoms.

The positions for the H atoms attached to the TETN molecule were initially calculated. Subsequently, those attached to carbon atoms were fixed during structural refinements and their positions updated based upon the refined parameters of the C atoms. The positions for the H atoms attached to the terminal nitrogen (N(1) in Fig. 2) were allowed to vary and converged to a stable and chemically reasonable minimum (Tables 2 and 3). Intramolecular hydrogen bonding is probably responsible for

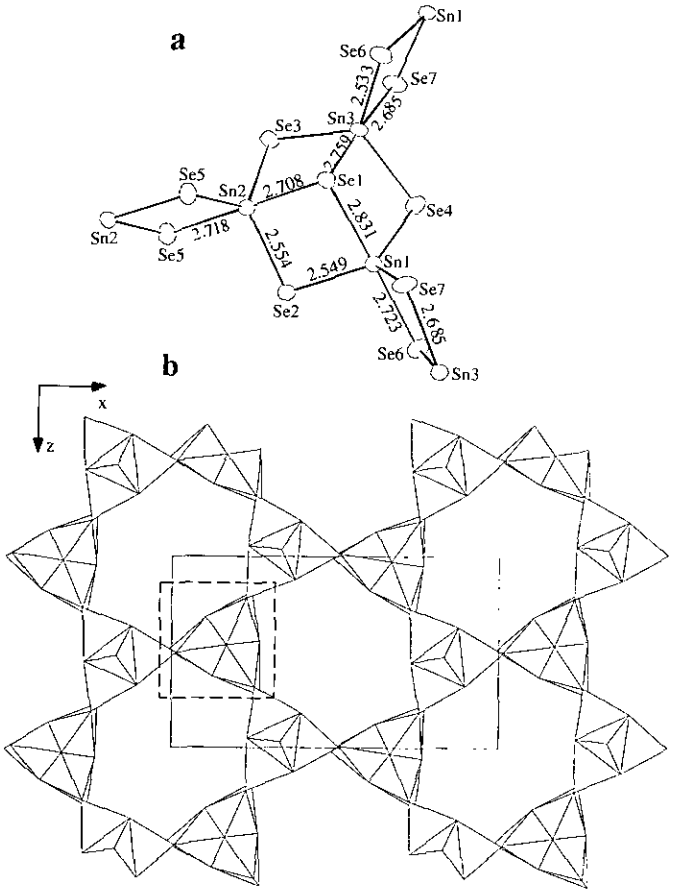

FIG. 1. (a) ORTEP (62) representation of the structure of the primary building unit (PBU) and of (b) the $Sn_3Se_7^{2-}$-layer of the TETN-SnSe-1, with the PBU, with a similar orientation to that shown in (a) outlined. In the latter diagram the $SnSe_5$-trigonal bipyramidal coordination polyhedra are used to construct the framework. The origin of the unit cell is in the top left corner with the a-axial direction to the right, c down, and b out of the plane of the paper. Interatomic distances and angles are given in Table 3. Errors on the interatomic distances given in (a) are 0.002 Å.

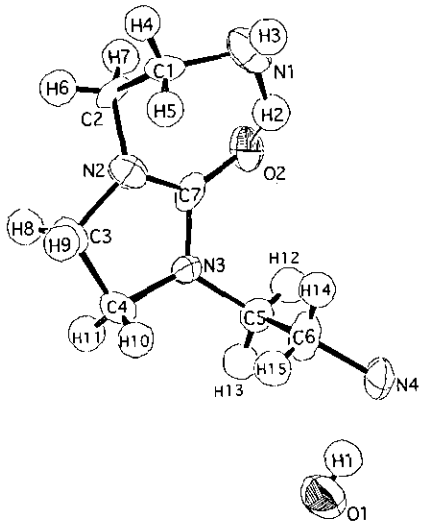

FIG. 2. The conformation of the 1,3-diaminoethyl-2-imidazolidone (TETN-CO) molecule found in the structure of TETN–SnSe-1. One end of the molecule forms a intermolecular H bond, N(1)–H(1) · · ·O(2).

the ordering of H on this terminal group; unfortunately no H atoms could be located on N(4), the other terminal nitrogen. This makes the allocation of charge between the template and the SnSe framework ambiguous since charge-compensating H^+ might be attached to either $Sn_3Se_7^{2-}$, $C_7H_{16}N_4O$, or H_2O. Subsequent Fourier difference calculations suggested the location of extra scattering, which was assigned to an oxygen atom (O(1) in Tables 2 and 3 and Fig. 2). The final refined parameters are given in Tables 1 and 2 with selected interatomic distances and angles given in Table 3.

TMA–SnOS-SB3. This framework type forms as an intermediate in both the transformation of TMA–SnS-1 and TETN–SnS-1 to the 4-connected SnOS framework (1). Initially, good single crystals of only the TMA phase were available and data were collected on these samples. The structure was solved using a combination of an automated Patterson search routine (56) and Fourier difference synthesis. The SnOS framework (Figs. 4 and 5), has composition $[Sn_{20}S_{37}O_8]^{10-}$ and was quite easily resolved (Fig. 3); however, the location of the interframework cations proved problematic.

Fourier difference calculations revealed only isolated peaks and "V"-shaped moieties suggestive of $N(CH_3)_2$ groups. In an attempt to better resolve the nature of the material occluded by framework, two data sets were collected on different diffractometers on crystals from different synthetic runs. Both crystals gave identical unit cell parameters, within experimental error (Table 1). Full structure analysis also gave the same results; a well-resolved framework but with poorly resolved scattering matter between the layers of the structure (Figs. 4 and 5). The results for one structure analysis are presented in Table 4; only those scattering sites common to Fourier difference maps calculated from the two sets of data were accepted. These peaks were then assigned carbon scatter-

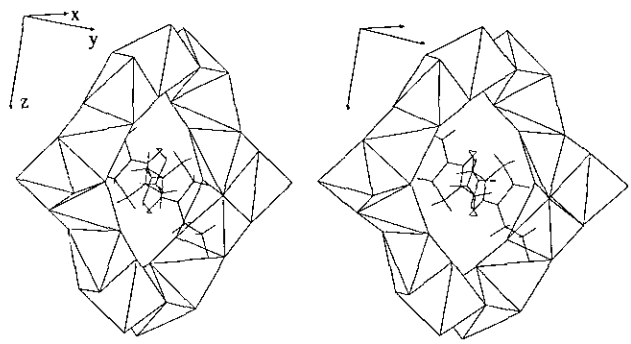

FIG. 3. Stereo view of the relationship between the TETN-CO molecule and the $Sn_3Se_7^{2-}$-framework in TETN–SnSe-1.

TABLE 2
Fractional Coordinates ($\times 10^4$) and Isotropic Thermal Parameters ($Å^2$) for TETN–SnSe-1§

atom	x	y	z	Biso
Sn(1)	2212.5(4)	-195.6(7)	5931.6(7)	1.9(0)'
Sn(2)	779.7(4)	-89.5(7)	4828.7(7)	1.8(0)'
Sn(3)	2035.6(4)	-64.5(7)	3232.3(7)	1.8(0)'
Se(1)	1673(1)	1119(1)	4688(1)	1.9(0)'
Se(2)	1238(1)	-913(1)	6265(1)	2.4(0)'
Se(3)	1032(1)	-789(1)	3184(1)	2.0(0)'
Se(4)	2682(1)	-917(1)	4452(1)	2.3(0)'
Se(5)	117(1)	1307(1)	5073(1)	2.1(0)'
Se(6)	2281(1)	1379(1)	2221(1)	2.2(0)'
Se(7)	2567(1)	1224(1)	6856(1)	2.3(0)'
O(1)	264(8)	1511(9)	2549(10)	6.2(5)'
O(2)	-622(5)	784(8)	1545(8)	3.6(3)'
N(1)	-1544(8)	1986(16)	1339(12)	4.4(6)'
N(2)	-908(6)	553(9)	8(10)	3.2(4)'
N(3)	-553(6)	-666(9)	786(9)	2.9(4)'
N(4)	-1011(6)	-2066(10)	2957(9)	3.6(4)'
C(1)	-1628(7)	1805(11)	279(12)	2.9(5)'
C(2)	-1079(7)	1533(11)	-202(12)	3.3(5)'
C(3)	-919(7)	-207(11)	-729(12)	3.0(5)'
C(4)	-738(7)	-1101(11)	-127(12)	2.9(5)'
C(5)	-486(7)	-1249(11)	1648(11)	3.1(5)'
C(6)	-1067(7)	-1525(13)	2051(12)	3.9(5)'
C(7)	-697(7)	281(12)	824(12)	2.8(5)'
H(1)¶	-307(74)	-3033(114)	2693(121)	3
H(2)¶	-1276(57)	1221(99)	1672(100)	3
H(3)¶	-1709(90)	2145(162)	1539(134)	3
H(4)*	-1777	2363	-15	3
H(5)*	-1898	1308	193	3
H(6)*	-1116	1612	-874	3
H(7)*	-788	1959	-5	3
H(8)*	-639	-79	-1200	3
H(9)*	-1297	-291	-952	3
H(10)*	-1059	-1495	-16	3
H(11)*	-423	-1403	-426	3
H(12)*	-280	-898	2116	3
H(13)*	-279	-1810	1495	3
H(14)*	-1285	-965	2161	3
H(15)*	-1265	-1903	1595	3

§ Space group *Pbca*, No. 61; all atoms on site 8c with full occupancy.

' Equivalent isotropic thermal parameter calculated: $B_{eq} = (8\pi^2/3)\ \Sigma_i \Sigma_j\ u_{ij} a_i^* a_j^* \vec{a}_i \vec{a}_j$.

¶ *Positions of H atoms refined; thermal parameters fixed and not refined.*

* Positions of H atoms calculated assuming ideal hydrocarbon geometry; thermal parameter fixed.

ing factors and their positional and thermal parameters were refined (Table 4). The unresolved nature of the occluded cations makes it difficult to assign the charge distribution between the SnOS layers (Fig. 4) and these organic species.

RESULTS AND DISCUSSION

The Structure of TETN–SnSe-1

The structure of the $Sn_3Se_7^{2-}$ framework found in TETN–SnSe-1 is similar to those found for other compounds in this series (33–39, 41, 46, 50). It consists of semicube clusters (44–46, 50, 51) containing three atoms of Sn which are 5-coordinated to Se with approximately trigonal bipyramidal geometry (Fig. 1 and Table 3). This structural unit would be a complete Sn_3S_4 cube but for the Sn vacancy at one cube corner (Fig. 1); hence the designation "semi cube." All Se are coordinated to two Sn, except Se(1). The 3-coordination of Se(1) results in axial interatomic distances, which are elongated by some 0.15 Å compared to the equatorial Sn–Se distances in the $SnSe_5$-trigonal bipyramid (Fig. 1 and Table 3). A unit similar in geometry to this exists in the structure of TMA–SnS-1 (50) and the layered materials related to it (33, 37–39, 53).

The Sn–Se semicubes are connected via Se_2 bridges to form sheets (Figs. 1 and 3) in (010)-containing apertures bounded by six such structural elements (Fig. 1). These sheets are stacked along [010] with consecutive layers related by the *b*- and *c*-glides; this incorporates a half-

TABLE 3
Selected Interatomic Distances[a] (Å) and Angles (°) for TETN–SnSe-1

Sn(1)-Se(1)	2.831 (2)	O(2)-C(7)	1.242 (18)
Sn(1)-Se(2)	2.549 (2)	O(1)-H(1)d	0.729 (152)
Sn(1)-Se(4)	2.552 (2)	N(1)-C(1)	1.515 (23)
Sn(1)-Se(6)a	2.723 (2)	N(2)-C(2)	1.460 (20)
Sn(1)-Se(7)	2.514 (2)	N(2)-C(3)	1.482 (19)
Sn(2)-Se(1)	2.708 (2)	N(2)-C(7)	1.301 (19)
Sn(2)-Se(2)	2.554 (2)	N(3)-C(4)	1.479 (20)
Sn(2)-Se(3)	2.567 (2)	N(3)-C(5)	1.462 (19)
Sn(2)-Se(5)b	2.718 (2)	N(3)-C(7)	1.370 (20)
Sn(2)-Se(5)	2.525 (2)	N(4)-C(6)	1.480 (20)
Sn(3)-Se(1)	2.759 (2)	N(1)-H(2)	1.327 (142)
Sn(3)-Se(3)	2.574 (2)	N(1)-H(3)	0.529 (215)
Sn(3)-Se(4)	2.578 (2)	C(1)-C(2)	1.505 (22)
Sn(3)-Se(6)	2.533 (2)	C(3)-C(4)	1.567 (22)
Sn(3)-Se(7)c	2.685 (2)	C(5)-C(6)	1.530 (23)
Se(1)-Sn(1)-Se(2)	87.98 (6)	C(2)-N(2)-C(3)	122 (1)
Se(1)-Sn(1)-Se(4)	87.43 (6)	C(2)-N(2)-C(7)	124 (1)
Se(1)-Sn(1)-Se(6)a	176.32 (8)	C(3)-N(2)-C(7)	114 (1)
Se(1)-Sn(1)-Se(7)	87.11 (6)	C(4)-N(3)-C(5)	121 (1)
Se(2)-Sn(1)-Se(4)	112.46 (6)	C(4)-N(3)-C(7)	111 (1)
Se(2)-Sn(1)-Se(6)a	91.94 (6)	C(5)-N(3)-C(7)	122 (1)
Se(2)-Sn(1)-Se(7)	121.13 (7)	C(1)-N(1)-H(2)	106 (6)
Se(4)-Sn(1)-Se(6)a	95.99 (6)	C(1)-N(1)-H(3)	119 (25)
Se(4)-Sn(1)-Se(7)	125.84 (7)	H(2)-N(1)-H(3)	120 (23)
Se(6)a-Sn(1)-Se(7)	89.79 (6)	O(2)-C(7)-N(2)	127 (2)
Se(1)-Sn(2)-Se(2)	90.61 (6)	O(2)-C(7)-N(3)	123 (1)
Se(1)-Sn(2)-Se(3)	89.66 (6)	N(2)-C(7)-N(3)	110 (1)
Se(1)-Sn(2)-Se(5)b	178.7 (1)	N(1)-C(1)-C(2)	111 (1)
Se(1)-Sn(2)-Se(5)	90.37 (6)	N(2)-C(2)-C(1)	113 (1)
Se(2)-Sn(2)-Se(3)	115.67 (7)	N(2)-C(3)-C(4)	101 (1)
Se(2)-Sn(2)-Se(5)	120.32 (6)	N(3)-C(4)-C(3)	102 (1)
Se(2)-Sn(2)-Se(5)b	90.31 (6)	N(3)-C(5)-C(6)	110 (1)
Se(3)-Sn(2)-Se(5)b	89.16 (6)	N(4)-C(6)-C(5)	111 (1)
Se(3)-Sn(2)-Se(5)	124.00 (6)		
Se(5)-Sn(2)-Se(5)b	89.91 (6)	Intramolecular Non-Bonding Distances (A)	
Se(1)-Sn(3)-Se(3)	88.40 (5)		
Se(1)-Sn(3)-Se(4)	88.50 (6)	O(2)...N(1)	2.762 (26)
Se(1)-Sn(3)-Se(6)	90.13 (6)	O(2)...C(1)	3.284 (19)
Se(1)-Sn(3)-Se(7)c	177.4 (1)	O(2)...C(6)	3.473 (21)
Se(3)-Sn(3)-Se(4)	112.17 (6)	O(2)...H(2)	1.668 (138)
Se(3)-Sn(3)-Se(6)	120.60 (6)	N(1)...C(7)	3.193 (28)
Se(3)-Sn(3)-Se(7)c	93.63 (6)		
Se(4)-Sn(3)-Se(6)	127.15 (7)	Intermolecular Distances (A)	
Se(4)-Sn(3)-Se(7)c	89.24 (6)		
Se(6)-Sn(3)-Se(7)c	90.23 (6)	Se(2)...O(2)b	3.389 (11)
Sn(1)-Se(1)-Sn(2)	84.14 (5)	O(1)...O(2)	2.713 (20)
Sn(1)-Se(1)-Sn(3)	85.57 (6)	O(1)...N(4)d	2.750 (20)
Sn(2)-Se(1)-Sn(3)	85.31 (5)	O(1)...C(5)d	3.372 (21)
Sn(1)-Se(2)-Sn(2)	93.36 (6)	O(1)...C(6)d	3.383 (23)
Sn(2)-Se(3)-Sn(3)	92.20 (6)		
Sn(1)-Se(4)-Sn(3)	95.50 (6)		
Sn(2)-Se(5)-Sn(2)b	90.09 (6)		
Sn(1)c-Se(6)-Sn(3)	89.02 (6)		
Sn(1)-Se(7)-Sn(3)a	90.29 (6)		

Note. Symmetry: (a) $1/2 - X, -Y, 1/2 + Z$; (b) $-X, -Y, 1 - Z$; (c) $1/2 - X, -Y, -1/2 + Z$; (d) $-X, 1/2 + Y, 1/2 - Z$.

[a] C–H distances fixed at 0.950 Å for H(4)–H(15).

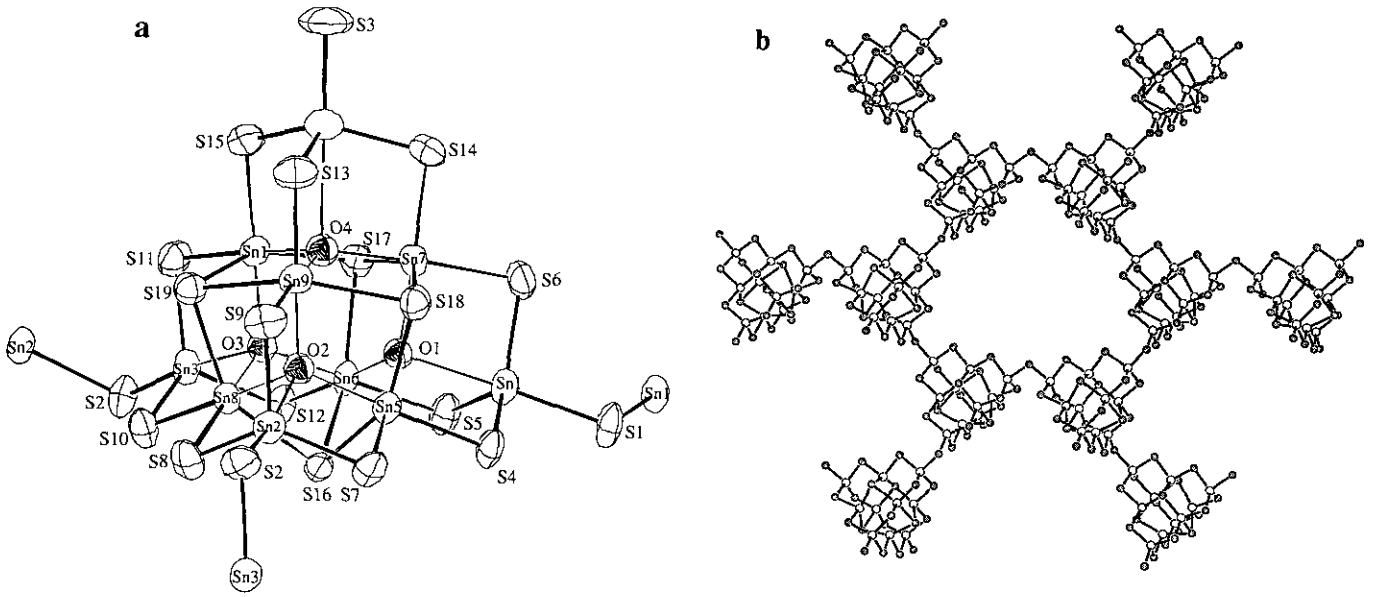

FIG. 4. (a) ORTEP (62) representation of the $[Sn_{10}S_{20}O_4]^{4-}$ building unit found in TMA–SnOS-SB3. The selected interatomic distances and angles are given in Table 5. The clusters outline apertures composed of six clusters in the SnOS sheet of TMA–SnOS-SB3 depicted in (b) as a CHARON drawing (molecular graphics program written by Joseph Lauher, SUNY, Stony Brook). For the sake of clarity the oxygen atoms within the cluster (a) are omitted from the representation of the sheet.

unit-cell translation parallel to either the *b*- or *c*-axes. The apertures of consecutive layers are thereby eclipsed by the next layer along [010]. The 1,3-diaminoethyl-2-imidazolidone molecule, produced during the formation of TETN–SnS-1 (55), resides within the apertures formed by the $Sn_3Se_7^{2-}$-framework. This is in contrast to the location of TMA^+ in TMA–SnS-1 (50) which resides *between* the layers. TMA–SnS-1 is a closely related structure type with a similar connectivity of semicubes but with different stacking of these layers; the distance between the centers of the layers along [010] is 7 Å in TETN–SnSe-1 compared to a distance of 8.5 Å found in the TMA–SnS-1 analog (50).

Apart from the larger separation between layers, the apertures in the TMA–SnS-1 are only partially eclipsed by adjacent layers (50). This, along with the positioning of the template molecule outside, rather than inside, the apertures (Fig. 3) suggests TMA–SnS-1 should be the better ion exchanger. Indeed preliminary experiments (50) confirmed that TMA^+ can be exchanged for a large variety of transition metal, main group metal, and alkylammonium cations. Our efforts to ion-exchange the TETN–SnSe framework have to date not been successful.

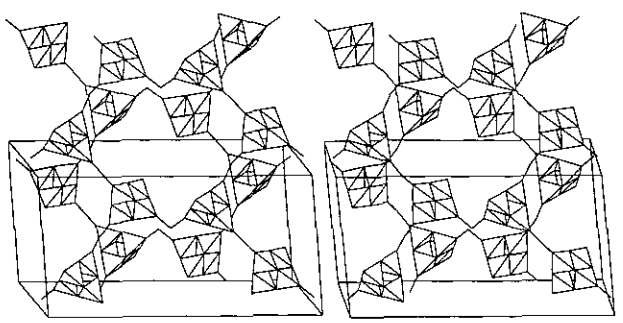

FIG. 5. Stereo view of the structure of TMA–SnOS-SB3. The origin of the unit cell is at the top front left hand corner with the *a*-axis to the right, the *b*-axial direction down, and the *c*-direction into the page. The corners of the tetrahedra constituting the clusters (Fig. 4) represent the positions of the tin atoms with S and O within the clusters omitted for clarity. In this representation, the S atoms are at the bends of the "elbow" joints between clusters.

The Structure of TMA–SnOS-SB3

The structure of the SnOS–SB3 framework consists of clusters (Fig. 4) of composition $(Sn_{10}S_{20}O_4)^{8-}$ which are 3-connected to each other via sulfur bridges (Fig. 5). The clusters can be thought of as supertetrahedra, which are linked at three corners (Fig. 4) in a fashion reminiscent of the tetrahedral (T) sheets found in the clays and micas (3). This leads to an overall composition of $(Sn_{20}S_{37}O_8)^{10-}$ for the sheet, presuming the nominal oxidation state of tin is +4 and that the sheet is not protonated.

A major difference between the layer silicates and the present material is the disposition of the tetrahedral units in the sheet. The tetrahedra in the 6-rings of the aluminosilicate biotite mica for example, are constrained to point

TABLE 4
Fractional Coordinates ($\times 10^4$) and Isotropic Thermal Parameters ($Å^2$) for TMA–SnOS-SB3[§]

atom	x	y	z	Biso
Sn(1)	465(0)	1382(1)	7201(1)	4.0(1)'
Sn(2)	2144(0)	645(1)	6378(1)	4.1(1)'
Sn(3)	2905(0)	-1082(1)	6984(1)	4.1(1)'
Sn(4)	646(0)	3415(1)	4521(1)	5.5(1)'
Sn(5)	1307(0)	1003(1)	6795(1)	3.7(1)'
Sn(6)	1280(0)	2648(1)	7625(1)	3.6(1)'
Sn(7)	571(0)	2380(1)	5907(1)	4.2(1)'
Sn(8)	2128(0)	2280(1)	7209(1)	3.5(0)'
Sn(9)	1410(0)	2015(1)	5497(1)	4.1(1)'
Sn(10)	3610(0)	-1355(1)	8682(1)	4.0(1)'
S(1)	0	660(4)	7500	5.4(4)'
S(2)	2532(2)	-243(3)	6066(3)	5.0(2)'
S(3)	283(3)	3959(4)	3477(4)	9.2(3)'
S(4)	851(2)	324(3)	7161(3)	4.7(2)'
S(5)	808(2)	2213(3)	8109(3)	4.7(2)'
S(6)	4(2)	1912(3)	6152(3)	5.4(2)'
S(7)	1708(2)	-64(3)	6729(3)	4.6(2)'
S(8)	2653(2)	1391(3)	7228(3)	5.0(2)'
S(9)	1829(2)	1118(3)	5245(3)	5.2(2)'
S(10)	2370(2)	-1905(3)	6944(3)	4.8(2)'
S(11)	3214(2)	-338(3)	7965(3)	4.8(2)'
S(12)	3345(2)	-1497(3)	6474(3)	4.7(2)'
S(13)	1063(2)	2483(3)	4343(3)	5.9(2)'
S(14)	119(2)	2909(3)	4815(3)	6.1(2)'
S(15)	1057(2)	4362(3)	5281(3)	5.8(2)'
S(16)	1820(1)	1591(2)	7937(2)	3.5(2)'
S(17)	786(1)	3528(3)	6696(3)	4.3(2)'
S(18)	820(2)	1195(3)	5530(3)	4.5(2)'
S(19)	1979(2)	3000(3)	6108(3)	4.2(1)
O(1)	971(3)	1929(6)	6831(5)	3.3(2)
O(2)	1683(3)	1613(6)	6466(6)	3.7(3)
O(3)	1677(3)	3001(6)	7191(6)	3.5(2)
O(4)	1078(4)	2741(6)	5773(6)	4.1(3)
C(1)	3470(23)	5657(39)	5623(36)	12.4(21)
C(2)	3908(30)	5499(50)	5439(48)	16.1(29)
C(3)	4063(24)	5535(42)	5070(41)	12.9(23)
C(4)	1913(22)	3668(41)	4318(36)	13.1(22)
C(5)	2180(21)	2796(37)	4393(34)	11.7(19)
C(6)	3122(25)	4417(44)	6554(39)	14.1(24)
C(7)	269(14)	6051(26)	3303(24)	6.6(11)
C(8)	0	6160(30)	2500	13.8(17)
C(9)	950(17)	4680(30)	2410(27)	8.6(14)
C(10)	4886(26)	6242(45)	3530(43)	15.0(26)

§ Space group $C2/c$, No. 15; all atoms on site 8*f* except S(1) and C(8) on site 4*e*.

' Equivalent isotropic thermal parameter calculated from anisotropic values for Sn and S atoms: $B_{eq} = (8\pi^2/3)\,\Sigma_i\,\Sigma_j\,u_{ij}a_i^*a_j^*\vec{a}_i\vec{a}_j$.

in the same direction, forming an UUUUUU array of tetrahedral bonding with AlO-octahedral layers in this mineral. In TMA–SnOS-SB3 the supertetrahedra adopt a chair conformation, UDUDUD, of nonbridging apices (Figs. 4 and 5). This conformation is also adopted in TETN–SnOS-SB2, the 4-connected three-dimensional framework composed of SnOS-supertetrahedra and related to the structure of cristobalite (1). Indeed the disposition of the nonbridging S3 atom, pointing toward the 6-ring opening in the sheet (Figs. 4 and 5), is suggestive of the structure of TETN–SnOS-SB2 in which six rings in successive layers are connected to produce two nonintersecting networks (1).

All Sn atoms in the main building unit of the structure are 4-coordinated to S in approximately tetrahedral arrangements forming a single ABC stacking sequence of the ZnS (zinc-blende) structure type (57) (Fig. 4a and Table 5). Oxygen is inserted into the tetrahedral sites with four atoms of tin at the corners. The oxygen is shifted from the center of the OSn_4 tetrahedron toward the center of the cluster (Fig. 4a) with three O–Sn distances of about 2.10 Å and one of greater than 2.45 Å (Fig. 4a and Table 5). In order to simplify depiction of the full structure, the $(Sn_{10}S_{20}O_4)^{8-}$ cluster can be reduced to the cubic close-packed array of metal atoms shown in Fig. 2. In this representation each cluster is connected at three of the four corners by Sn(3)–S(2)–Sn(2) and Sn(1)–S(1)–Sn(1) bridges to three other symmetry related clusters (Figs. 4 and 5). This angle is 111(2)° compared with a value of 113.1(6)° in the case of the 4-connected TETN–SnOS-SB2(1). This small angular variation in the sulfides and a correspondingly larger variation in silicate structure types are documented in recent theoretical treatments (58, 59).

Structural Evolution

Two routes have now been found to lead to structures containing the 3- and 4-connected oxy-sulfide clusters in the -SB3 and SB2 (1) frameworks, respectively. Both involve the initial crystallization of a sulfide framework from which oxy-sulfides develop. The source of oxygen for this reaction is as yet unknown. We have performed experiments in which starting materials were carefully purged of entrained oxygen. This suggests the source might be from decomposition of the water added as solvent; the reactions in the $S–H_2O$ and alkali-$S–H_2O$ systems leading to the formation of thio-sulfate have been known for sometime (60, 61). We are planning to follow these reactions using gas chromatography in order to better understand the role of oxygen in processes leading to the formation of oxy-sulfides in our systems.

Although structural details are not available on all of the intermediates involved, sufficient details have been determined to venture a scheme of structural evolution from the first materials to crystallize, SnS-1 or SnSe-1, to the last structure type observed (SnOS–SB2). In the case of the TMA–SnS system, the structural evolution follows the following scheme:

TMA–SnS-1 (50) → **TMA–SnS-1a** (51) →
TMA–SnOS-SB3 → TMA–SnOS-SB2. [1]

The structures determined in this sequence are in bold type. The organic compounds found in scheme 1 are:

$$(CH_3)_4N \rightarrow (CH_3)_3N \rightarrow (CH_3)_2N \rightarrow ? \qquad [2]$$

Similar sequences have been observed for TETN:

TETN–SnS-1 → TETN–SnOS-SB3 →
TETN–SnOS-SB2 (1). [3]

(Although the structure of TETN–SnS-1 has not been determined directly because of a lack of suitable single crystals, calculations of the powder diffraction pattern, based on the structure of the TETN–SnSe-1 given in Table 2, suggest that SnS-1 and SnSe-1 are isomorphous.)

The following organic molecules have been identified:

$$\text{TETN–C=O (Fig. 2)} \rightarrow ? \rightarrow (NH_2)_2C{=}O. \quad [4]$$

Despite the large unit cell volume and low density for the SnOS–SB3 materials (Table 1), it may be worthwhile collecting data at low temperature in order to attempt resolution of the occluded species. This would be particularly interesting in the case of the TETN material since the end-members of the transformation from layered sulfide

TABLE 5
Selected Interatomic Distances[a] (Å) and Angles (°) for TMA–SnOS-SB3

Sn(1)-S(1)	2.424 (4)	S(1)-Sn(1)-S(4)	91.7 (2)
Sn(1)-S(4)	2.412 (5)	S(1)-Sn(1)-S(5)	107.1 (2)
Sn(1)-S(5)	2.389 (6)	S(1)-Sn(1)-S(6)	102.5 (1)
Sn(1)-S(6)	2.383 (6)	S(4)-Sn(1)-S(5)	117.0 (2)
Sn(2)-S(2)	2.423 (5)	S(4)-Sn(1)-S(6)	117.8 (2)
Sn(2)-S(7)	2.395 (5)	S(5)-Sn(1)-S(6)	115.6 (2)
Sn(2)-S(8)	2.398 (6)	S(2)-Sn(2)-S(7)	104.3 (2)
Sn(2)-S(9)	2.403 (6)	S(2)-Sn(2)-S(8)	106.0 (2)
Sn(3)-S(2)	2.431 (6)	S(2)-Sn(2)-S(9)	91.6 (2)
Sn(3)-S(10)	2.407 (5)	S(7)-Sn(2)-S(8)	116.4 (2)
Sn(3)-S(11)	2.383 (6)	S(7)-Sn(2)-S(9)	116.6 (2)
Sn(3)-S(12)	2.407 (5)	S(8)-Sn(2)-S(9)	117.0 (2)
Sn(4)-S(3)	2.315 (6)	S(2)-Sn(3)-S(10)	103.2 (2)
Sn(4)-S(13)	2.413 (6)	S(2)-Sn(3)-S(11)	104.7 (2)
Sn(4)-S(14)	2.417 (6)	S(2)-Sn(3)-S(12)	93.1 (2)
Sn(4)-S(15)	2.425 (6)	S(10)-Sn(3)-S(11)	116.8 (2)
Sn(5)-S(4)	2.443 (5)	S(10)-Sn(3)-S(12)	116.4 (2)
Sn(5)-S(7)	2.473 (5)	S(11)-Sn(3)-S(12)	117.3 (2)
Sn(5)-S(16)	2.615 (5)	S(3)-Sn(4)-S(13)	105.8 (3)
Sn(5)-S(18)	2.582 (6)	S(3)-Sn(4)-S(14)	105.1 (3)
Sn(6)-S(5)	2.475 (5)	S(3)-Sn(4)-S(15)	106.3 (2)
Sn(6)-S(12)b	2.429 (5)	S(13)-Sn(4)-S(14)	111.7 (2)
Sn(6)-S(16)	2.616 (5)	S(13)-Sn(4)-S(15)	113.0 (2)
Sn(6)-S(17)	2.608 (5)	S(14)-Sn(4)-S(15)	114.0 (2)
Sn(7)-S(6)	2.460 (5)	S(4)-Sn(5)-S(7)	95.3 (2)
Sn(7)-S(14)	2.440 (6)	S(4)-Sn(5)-S(16)	101.0 (2)
Sn(7)-S(17)	2.632 (5)	S(4)-Sn(5)-S(18)	100.7 (2)
Sn(7)-S(18)	2.622 (5)	S(7)-Sn(5)-S(16)	101.6 (2)
Sn(8)-S(8)	2.475 (5)	S(7)-Sn(5)-S(18)	100.8 (2)
Sn(8)-S(10)b	2.459 (6)	S(16)-Sn(5)-S(18)	147.0 (2)
Sn(8)-S(16)	2.618 (5)	S(5)-Sn(6)-S(12)b	95.9 (2)
Sn(8)-S(19)	2.597 (5)	S(5)-Sn(6)-S(16)	101.8 (2)
Sn(9)-S(9)	2.445 (5)	S(5)-Sn(6)-S(17)	100.4 (2)
Sn(9)-S(13)	2.443 (6)	S(12)b-Sn(6)-S(16)	100.7 (2)
Sn(9)-S(18)	2.615 (5)	S(12)b-Sn(6)-S(17)	100.3 (2)
Sn(9)-S(19)	2.624 (5)	S(16)-Sn(6)-S(17)	147.5 (2)
Sn(10)-S(11)	2.466 (5)	S(6)-Sn(7)-S(14)	95.4 (2)
Sn(10)-S(15)c	2.448 (6)	S(6)-Sn(7)-S(17)	100.1 (2)
Sn(10)-S(17)c	2.621 (5)	S(6)-Sn(7)-S(18)	101.2 (2)
Sn(10)-S(19)c	2.619 (5)	S(14)-Sn(7)-S(17)	101.7 (2)
Sn(1)-O(1)	2.48 (1)	S(14)-Sn(7)-S(18)	101.4 (2)
Sn(2)-O(2)	2.49 (1)	S(17)-Sn(7)-S(18)	146.7 (2)
Sn(3)-O(3)c	2.46 (1)	S(8)-Sn(8)-S(10)b	95.3 (2)
Sn(5)-O(1)	2.11 (1)	S(8)-Sn(8)-S(16)	100.2 (2)
Sn(5)-O(2)	2.10 (1)	S(8)-Sn(8)-S(19)	102.0 (2)
Sn(6)-O(1)	2.08 (1)	S(10)b-Sn(8)-S(16)	101.5 (2)
Sn(6)-O(3)	2.11 (1)	S(10)b-Sn(8)-S(19)	100.3 (2)
Sn(7)-O(1)	2.08 (1)	S(16)-Sn(8)-S(19)	147.1 (2)
Sn(7)-O(4)	2.06 (1)	S(9)-Sn(9)-S(13)	95.4 (2)
Sn(8)-O(2)	2.11 (1)	S(9)-Sn(9)-S(18)	100.9 (2)
Sn(8)-O(3)	2.07 (1)	S(9)-Sn(9)-S(19)	99.9 (2)
Sn(9)-O(2)	2.05 (1)	S(13)-Sn(9)-S(18)	100.2 (2)
Sn(9)-O(4)	2.04 (1)	S(13)-Sn(9)-S(19)	102.6 (2)
Sn(10)-O(3)c	2.10 (1)	S(18)-Sn(9)-S(19)	147.4 (2)
Sn(10)-O(4)c	2.08 (1)	S(11)-Sn(10)-S(15)c	95.4 (2)
Sn(4)-O(4)c	2.79(1)	S(11)-Sn(10)-S(17)c	100.8 (2)
C(7)-C(8)	1.61 (5)	S(11)-Sn(10)-S(19)c	100.0 (2)
		S(15)c-Sn(10)-S(17)c	101.5 (2)
S(1)-Sn(1)-O(1)	170.5 (3)	S(15)c-Sn(10)-S(19)c	100.9 (2)
S(4)-Sn(1)-O(1)	79.2 (3)	S(17)c-Sn(10)-S(19)c	147.6 (2)
S(5)-Sn(1)-O(1)	80.0 (3)		
S(6)-Sn(1)-O(1)	79.5 (3)	S(5)-Sn(6)-O(1)	86.3 (3)
S(2)-Sn(2)-O(2)	169.2 (3)	S(5)-Sn(6)-O(3)	178.6 (3)
S(7)-Sn(2)-O(2)	80.1 (3)	S(12)b-Sn(6)-O(1)	177.8 (4)
S(8)-Sn(2)-O(2)	80.3 (3)	S(12)b-Sn(6)-O(3)	85.6 (3)
S(9)-Sn(2)-O(2)	77.6 (3)	S(16)-Sn(6)-O(1)	79.0 (3)
S(2)-Sn(3)-O(3)c	171.9 (3)	S(16)-Sn(6)-O(3)	77.9 (3)
S(10)-Sn(3)-O(3)c	79.3 (3)	S(17)-Sn(6)-O(1)	79.0 (3)
S(11)-Sn(3)-O(3)c	80.6 (3)	S(17)-Sn(6)-O(3)	79.4 (3)
S(12)-Sn(3)-O(3)c	79.0 (3)	S(6)-Sn(7)-O(1)	86.1 (3)
S(4)-Sn(5)-O(1)	86.3 (3)	S(6)-Sn(7)-O(4)	175.6 (3)
S(4)-Sn(5)-O(2)	178.1 (4)	S(14)-Sn(7)-O(1)	178.5 (4)
S(7)-Sn(5)-O(1)	178.3 (4)	S(14)-Sn(7)-O(4)	89.1 (4)
S(7)-Sn(5)-O(2)	86.5 (3)	S(17)-Sn(7)-O(1)	78.5 (3)
S(16)-Sn(5)-O(1)	78.6 (3)	S(17)-Sn(7)-O(4)	78.8 (3)
S(16)-Sn(5)-O(2)	79.4 (3)	S(18)-Sn(7)-O(1)	77.8 (3)
S(18)-Sn(5)-O(1)	78.3 (3)	S(18)-Sn(7)-O(4)	78.0 (3)
S(18)-Sn(5)-O(2)	78.1 (3)	S(8)-Sn(8)-O(2)	86.4 (3)
		S(8)-Sn(8)-O(3)	178.3 (3)
Sn(1)-S(1)-Sn(1)a	113.3 (3)	S(10)b-Sn(8)-O(2)	178.0 (4)
Sn(2)-S(2)-Sn(3)	112.0 (2)	S(10)b-Sn(8)-O(3)	86.0 (3)
Sn(1)-S(4)-Sn(5)	93.7 (2)	S(16)-Sn(8)-O(2)	79.1 (3)
Sn(1)-S(5)-Sn(6)	93.0 (2)	S(16)-Sn(8)-O(3)	78.5 (3)
Sn(1)-S(6)-Sn(7)	93.5 (2)	S(19)-Sn(8)-O(2)	78.3 (3)
Sn(2)-S(7)-Sn(5)	93.1 (2)	S(19)-Sn(8)-O(3)	78.8 (3)
Sn(2)-S(8)-Sn(8)	93.1 (2)	S(9)-Sn(9)-O(2)	85.5 (3)
Sn(2)-S(9)-Sn(9)	94.3 (2)	S(9)-Sn(9)-O(4)	176.2 (4)
Sn(3)-S(10)-Sn(8)c	92.9 (2)	S(13)-Sn(9)-O(2)	178.3 (3)
Sn(3)-S(11)-Sn(10)	92.9 (2)	S(13)-Sn(9)-O(4)	88.4 (4)
Sn(3)-S(12)-Sn(6)c	94.1 (2)	S(18)-Sn(9)-O(2)	78.1 (3)
Sn(4)-S(13)-Sn(9)	99.2 (2)	S(18)-Sn(9)-O(4)	78.4 (3)
Sn(4)-S(14)-Sn(7)	98.7 (2)	S(19)-Sn(9)-O(2)	78.7 (3)
Sn(4)-S(15)-Sn(10)b	98.9 (2)	S(19)-Sn(9)-O(4)	79.2 (3)
Sn(5)-S(16)-Sn(6)	85.8 (1)	S(11)-Sn(10)-O(3)c	86.1 (3)
Sn(5)-S(16)-Sn(8)	85.7 (2)	S(11)-Sn(10)-O(4)c	175.9 (3)
Sn(6)-S(16)-Sn(8)	86.0 (1)	S(15)c-Sn(10)-O(3)c	178.2 (3)
Sn(6)-S(17)-Sn(7)	85.3 (1)	S(15)c-Sn(10)-O(4)c	88.6 (4)
Sn(6)-S(17)-Sn(10)b	85.7 (1)	S(17)c-Sn(10)-O(3)c	79.2 (3)
Sn(7)-S(17)-Sn(10)b	84.7 (2)	S(17)c-Sn(10)-O(4)c	78.8 (3)
Sn(5)-S(18)-Sn(7)	86.6 (2)	S(19)c-Sn(10)-O(3)c	77.7 (3)
Sn(5)-S(18)-Sn(9)	86.0 (2)	S(19)c-Sn(10)-O(4)c	78.7 (3)
Sn(7)-S(18)-Sn(9)	84.7 (2)		
Sn(8)-S(19)-Sn(9)	85.6 (2)	O(1)-Sn(5)-O(2)	91.9 (4)
Sn(8)-S(19)-Sn(10)b	86.1 (2)	O(1)-Sn(6)-O(3)	92.2 (4)
Sn(9)-S(19)-Sn(10)b	84.4 (2)	O(1)-Sn(7)-O(4)	89.5 (4)
		O(2)-Sn(8)-O(3)	92.3 (4)
Sn(1)-O(1)-Sn(5)	100.7 (4)	O(2)-Sn(9)-O(4)	90.7 (5)
Sn(1)-O(1)-Sn(6)	100.7 (4)	O(3)c-Sn(10)-O(4)c	89.9 (4)
Sn(1)-O(1)-Sn(7)	100.8 (4)		
Sn(5)-O(1)-Sn(6)	116.3 (5)	Intramolecular Non-Bonding Distances	
Sn(5)-O(1)-Sn(7)	116.8 (5)		
Sn(6)-O(1)-Sn(7)	116.8 (5)	Sn(5)...Sn(10)b	5.025 (2)
Sn(2)-O(2)-Sn(5)	100.4 (4)	Sn(6)...Sn(9)	5.004 (2)
Sn(2)-O(2)-Sn(8)	100.2 (4)	Sn(7)...Sn(8)	5.035 (2)
Sn(2)-O(2)-Sn(9)	102.5 (4)	S(7)...S(10)	4.050 (7)
Sn(5)-O(2)-Sn(8)	115.4 (5)	S(8)...S(11)	3.744 (7)
Sn(5)-O(2)-Sn(9)	117.1 (5)		
Sn(8)-O(2)-Sn(9)	116.8 (5)	Intermolecular Distances (Å)	
Sn(3)b-O(3)-Sn(6)	101.3 (4)		
Sn(3)b-O(3)-Sn(8)	101.9 (4)	C(1)...C(2)	1.790 (115)
Sn(3)b-O(3)-Sn(10)b	100.4 (4)	C(1)...C(3)	2.855 (107)
Sn(6)-O(3)-Sn(8)	117.1 (5)	C(4)...C(5)	1.842 (91)
Sn(6)-O(3)-Sn(10)b	115.0 (5)	C(5)...C(5)e	2.871 (135)
Sn(8)-O(3)-Sn(10)b	116.8 (5)		
Sn(7)-O(4)-Sn(9)	118.8 (6)		
Sn(7)-O(4)-Sn(10)b	117.7 (5)		
Sn(9)-O(4)-Sn(10)b	117.6 (5)		

[a] Symmetry: (a) $-x, y, 3/2 - z$; (b) $1/2 - x, 1/2 + y, 3/2 - z$; (c) $1/2 - x, -1/2 + y, 3/2 - z$; (d) $-x, y, 1/2 - z$; (e) $1/2 - x, 1/2 - y, 1 - z$.

SnS-1 to 4-connected SnOS–SB2 (I) are well known (schemes [3] and [4] above).

The structures of the two oxy-sulfides determined thus far are members of a hypothetical family of structures which can be constructed by corner-linking the supertetrahedral clusters shown in Fig. 4. In this regard the silicates can be instructive in predicting the structural chem-

istry which might be possible with this new class of materials. The oxy-sulfides belong to a hypothetical structural family with composition $[Sn_{10}S_{20-n/2}O_4]^{(8-n)-}$, where $0 \leq n \leq 4$ is the number of connections between clusters. As yet we have been unable to crystallize the selenium analogs. We have found the growth of single crystals of the tin thio-oxide benefit from hydrothermal treatment for extended periods. However, at least the isolated cluster can be prepared without prolonged heating (2) and it may be possible to produce other materials related to the oxy-sulfides described here, using milder conditions.

CONCLUSION

Three distinct structure types built from 3-connected (Fig. 2), 4-connected, and isolated SnOS supertetrahedral clusters have now been identified. These structures have been synthesized from a restricted range of temperatures, starting compositions, reaction times, and added organic amines. There is some potential for other novel connectivities in this system and synthetic strategies to produce them are being explored. The hydrothermal chemistry of the aluminosilicates may be a useful guide in this regard. The structural variations arising from the corner-sharing of tetrahedral moieties is well known (3, 22, 57). Thus far we have demonstrated that SnOS clusters can mimic characteristics of two of the five major silicate structural families; TMA–SnOS–SB3 contains 3-connected sheets found in the sheet or phyllo-silicates. TMA–SnOS–SB2 possesses the 4-connected framework reminiscent of the tectosilicates.

ACKNOWLEDGMENTS

This work is supported by NSF through Grants DMR-9413003 to J.B.P. The software used for the crystallographic calculations and depiction of the structures was developed and maintained by J. Calabrese of the DuPont Company and Joseph Lauher of the Department of Chemistry at Stony Brook.

REFERENCES

1. J. B. Parise and Y. Ko., *Chem. Mater.* **6,** 718 (1994).
2. B. Krebs, *Angew. Chem. Int. Ed. Engl.* **22,** 113 (1983).
3. F. Liebau, "Structural Chemistry of Silicates," p. 90. Springer-Verlag, Berlin, 1985.
4. R. M. Barrer, "Zeolites and Clay Minerals as Sorbents and Molecular Sieves," p. 1. Academic Press, London, 1978.
5. R. M. Barrer, *Zeolites* **1,** 130 (1981).
6. R. M. Barrer, "Hydrothermal Chemistry of Zeolites," p. 186. Academic Press, London/New York, 1982.
7. M. E. Davis and P. F. Lobo, *Chem. Mater.* **4,** 756 (1992).
8. T. W. Wilson, B. M. Lok, and E. M. Flanigen, U.S. Patent 4,310,440.
9. J. W. Richardson, Jr., J. V. Smith, and J. J. Pluth, *J. Phys. Chem.* **93,** 8212 (1989).
10. D. M. Poojary and A. Clearfield, *Zeolites* **13,** 542 (1993).
11. B. M. Lok, C. A. Messina, R. L. Patton, R. T. Gajek, T. R. Cannan, and E. M. Flanigen, U.S. Patent 4,440,871, 1984.
12. J. M. Bennett, W. J. Dytrych, J. J. Pluth, J. W. Richardson, and J. V. Smith, *Zeolites* **6,** 349 (1986).
13. M. Estermann, L. B. McCusker, C. Baerlocher, A. Merrouche, and H. Kessler, *Nature* **352,** 320 (1991).
14. J. B. Parise, *Inorg. Chem.* **24,** 4312 (1985).
15. T. E. Gier and G. D. Stucky, *Nature* **349,** 508 (1991).
16. D. M. Chapman and A. L. Roe, *Zeolites* **10,** 730,737 (1990).
17. R. C. Haushalter and F. W. Lai, *Angew. Chem. Int. Engl.* **28,** 743 (1989).
18. R. C. Haushalter and F. W. Lai, *J. Solid State Chem.* **83,** 202 (1989).
19. H. E. King, L. A. Mundi, K. G. Strohmaier, and R. C. Haushalter, *J. Solid State Chem.* **91,** 1 (1991).
20. V. Soghomonian, Q. Chen, R. C. Haushalter, and J. Zubieta, *Chem. Mater.* **5,** 1690 (1993).
21. A. Clearfield, "Proceedings, International Conference on Ion Exchange," p. 121. Kodansha, Tokyo, 1991.
22. A. F. Wells, "Further Studies of Three-Dimensional Nets," Am. Crystallog. Assoc. Monograph, Am. Crystallogr. Assoc., Buffalo, NY, 1979.
23. B. M. Lok, T. R. Cannan, and C. A. Messina, *Zeolites* **3,** 282 (1983).
24. G. D. Price, J. J. Pluth, J. V. Smith, and T. Araki, *Nature* **292,** 818 (1981).
25. H. Ray and A. Rabenau, *Solid State Commun.* **5,** 331 (1967).
26. W. M. Meier and D. H. Olson, "Atlas of Zeolite Structure Types," p. 100. Butterworths, London, 1987.
27. N. Herron, Y. Wang, M. M. Eddy, G. D. Stucky, D. E. Cox, K. Moller, and T. Bein, *J. Am. Chem. Soc.* **11,** 530 (1989).
28. G. A. Ozin, A. Kuperman, and A. Stein, *Angew. Chem. Int. Ed. Engl.* **28,** 359 (1989).
29. G. A. Ozin, S. Kirkby, M. Mezaros, S. Özkar, A. Stein, and G. D. Stucky, "Materials for Non-linear Optics, Chemical Perspectives," p. 554, 1990.
30. J. B. Parise, J. E. MacDougall, N. Herron, R. Farlee, A. W. Sleight, Y. Wang, T. Bein, K. Moller, and L. M. Moroney, *Inorg. Chem.* **27,** 221 (1988).
31. C. Bonifax, D. R. Corbin, and J. B. Parise, U.S. Patent 4,613,720, 1986.
32. B. Krebs, D. Voelker, and K. Stiller, *Inorg. Chem. Acta,* L101 (1982).
33. W. S. Sheldrick, *Z. Anorg. Allg. Chem.* **562,** 23 (1988).
34. W. S. Sheldrick and H. Häusler, *Z. Anorg. Allg. Chem.* **557,** 105 (1988).
35. W. S. Sheldrick and H. Häusler, *Z. Anorg. Allg. Chem.* **557,** 98 (1988).
36. W. S. Sheldrick and H. Häusler, *Z. Anorg. Allg. Chem.* **561,** 139 (1988).
37. W. S. Sheldrick, *Z. Naturforsch. B* **43,** 249 (1988).
38. W. S. Sheldrick and H. G. Braunbeck, *Z. Naturforsch. B* **44,** 851 (1989).
39. W. S. Sheldrick and H. G. Braunbeck, *Z. Naturforsch. B* **45,** 1643 (1989).
40. R. L. Bedard, S. T. Wilson, L. D. Vail, J. M. Bennett, and E. M. Flanigen, "Zeolites: Facts, Figures, Future" (P. A. Jacobs and R. A. Van Santen, Eds.), Studies in Surface Science & Catalysis, p. 375. Elsevier, Amsterdam, 1989.
41. R. L. Bedard, L. D. Vail, S. T. Wilson, and E. M. Flanigen, U.S. Patent 4,880,761, 1989.
42. R. L. Bedard, L. D. Vail, S. T. Wilson, and E. M. Flanigen, U.S. Patent 4,933,068, 1990.
43. J. B. Parise, *J. Chem. Soc. Chem. Commun.*, 1553 (1990).
44. J. B. Parise, *Science* **251,** 292 (1991).
45. J. B. Parise and Y. Ko, *Chem. Mater.* **4,** 1446 (1992).

46. Y. Ko, C. Cahill, and J. B. Parise, *J. Chem. Soc. Chem. Commun.*, 69 (1994).
47. D. J. Vaughan and J. R. Craig, "Mineral Chemistry of Metal Sulfides." Cambridge Univ. Press, Cambridge, 1978.
48. H. Geis and B. Marler, *Zeolites* **12,** 42 (1992).
49. L. E. Iton, F. Trouw, T. O. Brun, J. E. Epperson, J. W. White, and S. J. Henderson, *Langmuir* **8,** 1045 (1992).
50. J. B. Parise, Y. Ko, J. Rijssenbeek, D. M. Nellis, K. Tan, and S. Koch, *J. Chem. Soc. Chem. Commun.*, 527 (1994).
51. K. Tan, Y. Ko, and J. B. Parise, *Acta Crystallogr.* **C51,** 398 (1995).
52. S. Budavari, "The Merck Index," 7th ed., p. 9155. Merck, Rahway, NJ, 1989.
53. Y. Ko, K. Tan, D. M. Nellis, S. Koch, and J. B. Parise, *J. Solid State Chem.* **114,** 506 (1995).
54. K. Tan, Y. Ko, and J. B. Parise, *Acta Crystallogr.* **C50,** 1439 (1994).
55. J. F. Mulvaney and R. L. Evans, *Ind. Eng. Chem.* **40,** 393 (1948).
56. J. C. Calabrese, personal communication, 1994.
57. B. G. Hyde and S. Andersson, "Inorganic Crystal Structures." Wiley, New York, 1989.
58. K. L. Geisinger and G. V. Gibbs, *Phys. Chem. Miner.* **7,** 204 (1981).
59. G. V. Gibbs, *Am. Mineral.* **67,** 421 (1982).
60. R. H. Arntson, F. W. Dickson, and G. Tunell, *Science* **128,** 716 (1958).
61. R. H. Arntson, F. W. Dickson, and G. Tunell, *Am. J. Sci.* **258,** 574 (1960).
62. C. K. Johnson, "ORTEP: A Fortran Thermal-Ellipsoid Plot Program for Crystal Structure Illustration," ORNL Report 5138, Oak Ridge National Laboratory, Oak Ridge, TN, 1976.
63. N. Walker and D. Stuart, *Acta Crystallogr. Sect. A* **39,** 158 (1983).